

Annotation-Free Visual Reasoning for High-Resolution Large Multimodal Models via Reinforcement Learning

Jiacheng Yang^{1*}, Anqi Chen^{1*}, Yunkai Dang¹, Qi Fan¹, Cong Wang¹,
Wenbin Li^{1†}, Feng Miao², Yang Gao¹

¹School of Artificial Intelligence Science and Technology, Nanjing University

²School of Physics, Nanjing University

jiachengyang@smail.nju.edu.cn, liwenbin@nju.edu.cn

Abstract

Current Large Multimodal Models (LMMs) struggle with high-resolution visual inputs during the reasoning process, as the number of image tokens increases quadratically with resolution, introducing substantial redundancy and irrelevant information. A common practice is to identify key image regions and refer to their high-resolution counterparts during reasoning, typically trained with external visual supervision. However, such visual supervision cues require costly grounding labels from human annotators. Meanwhile, it remains an open question how to enhance a model’s grounding abilities to support reasoning without relying on additional annotations. In this paper, we propose **H**igh-resolution **A**nnotation-free **R**easoning **T**echnique (HART), a closed-loop framework that enables LMMs to focus on and self-verify key regions of high-resolution visual inputs. HART incorporates a post-training paradigm in which we design Advantage Preference Group Relative Policy Optimization (AP-GRPO) to encourage accurate localization of key regions. Notably, HART provides explainable reasoning pathways and enables efficient optimization of localization. Extensive experiments demonstrate that HART improves performance across a wide range of high-resolution visual tasks, consistently outperforming strong baselines. When applied to post-train Qwen2.5-VL-7B, HART even surpasses larger-scale models such as Qwen2.5-VL-72B and LLaVA-OneVision-72B on high-resolution, vision-centric benchmarks.

1. Introduction

Recent advances in Large Multimodal Models (LMMs) have attracted increasing attention from both industry and academia [3, 7, 10, 11, 17, 18]. LMMs have been widely

*Equal contribution.

†Corresponding author.

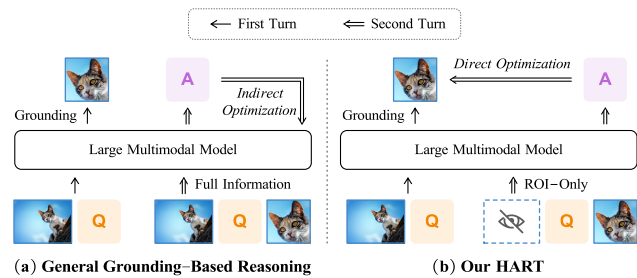


Figure 1. Optimization procedures of (a) general grounding-based methods without bounding-box annotations and (b) our proposed model. General models indirectly optimize grounding performance, while HART performs direct optimization by answering based solely on the ROIs. Abbreviations: Q—Question; A—Answer.

applied to complex real-world tasks, such as object detection [25, 29] and visual question answering [42, 50, 54]. They demonstrate strong capabilities in visual understanding and have the potential for enabling image-text interleaved reasoning. Despite these advances, current LMMs still face a critical limitation: their performance degrades significantly on challenging high-resolution visual tasks [15, 21, 58]. In such tasks, the number of visual tokens increases significantly with the resolution of the input images, while only a small subset contains key information. Popular LMM architectures, such as Qwen2.5-VL [3] and InternVL3 [66], typically impose a maximum pixel constraint on input images to address this issue. However, this constraint can lead to the loss of key information, restricting the model’s visual perception capability [2, 8, 28, 62].

To address this issue, existing works have explored a reasoning pathway that incorporates visual grounding, which is inspired by human visual processing [27, 52, 58]. Humans need to identify food and predators for survival in the wild, thus evolving the macula—a zone of acute vision in the retina [36]. This structure guides visual attention and eye movements to locate key regions within high-

resolution images. Previous works have developed visual grounded reasoning models, attempting to equip LMMs with similar structures and functions [30, 64]. Conditioned on the textual question, they first predict key regions of interest (ROI) with the downsampled image and then solve the question based on both the downsampled image and the ROIs from the original resolution. This pathway focuses only on critical visual information, thereby effectively reducing redundant computations. There are two lines of research that study the optimization of visual grounded reasoning models. On the one hand, some works directly enhance localization capabilities by using auxiliary visual annotations [32, 37, 39]. However, these methods require costly grounding labels from human annotators [48]. On the other hand, recent research leverages reinforcement learning (RL) [43] to jointly optimize grounding and reasoning without relying on additional annotated data [16, 41, 65]. These annotation-free approaches perform simple answer matching through a reward function. The model’s rewards measure the correctness of the final answer but cannot directly reflect localization accuracy. Specifically, the model receives a positive reward when the answer is correct, even if the localization is incorrect. Such reward misspecification will lead to negative optimization of grounding performance. In early attempts, we observed that this problem occurred in more than half of the cases (58% for Qwen2.5-VL-7B and 90% for InternVL3-8B). Therefore, it is natural to think: *How to directly optimize the grounding capabilities of LMMs without external visual annotations?*

To bridge this gap, this work aims to enable the model to self-verify its localization results for policy updates. In our design, after identifying the ROIs, the model answers based solely on the sub-regions and the original question. If the answer is correct, we consider that the ROIs contain the key visual information relevant to the question, indicating a faithful grounding. To this end, we propose a novel approach, *High-resolution Annotation-free Reasoning Technique (HART)*, to efficiently improve the performance of LMMs in high-resolution real-world scenarios without relying on extra visual annotations beyond final answers. We design a closed-loop framework to overcome the limitation imposed by resolution constraints. Given a textual question and a high-resolution image, our model identifies the ROIs and then crops relevant regions. These regions serve as visual feedback guiding the reasoning process. Subsequently, the original image is deliberately withheld, and the model answers the same question based solely on the cropped sub-images. In this way, the model can self-verify the grounding accuracy, since only ROIs containing key information lead to correct reasoning.

Based on the feedback loop, we introduce Advantage Preference Group Relative Policy Optimization (AP-GRPO), a reinforcement fine-tuning strategy that enables

the rewards to directly enhance grounding capabilities by introducing dynamic hyper-parameter adjustment. Figure 1 compares the procedures of general annotation-free grounding-based methods and our proposed method. Different from existing models [16, 65], HART can directly optimize visual grounding, thereby further enhancing the model’s performance on perception-heavy tasks. When applied to post-train Qwen2.5-VL-7B [3], HART even outperforms larger-scale models such as Qwen2.5-VL-72B [3] and LLaVA-OneVision-72B [20] on high-resolution, vision-centric benchmarks. The main contributions are summarized as follows:

- We develop HART, a novel and interpretable framework that enhances the joint understanding of visual and textual inputs. It enables direct optimization of visual grounding without additional manual annotations.
- We introduce a reinforcement fine-tuning strategy, termed AP-GRPO, within the post-training paradigm to better incentivize the model to focus on key regions by prioritizing samples with correct grounding.
- We validate our method’s effectiveness on several high-resolution visual benchmarks and show that HART achieves state-of-the-art performance among methods supervised only by the final answer.

2. Related Work

2.1. Large Multimodal Models

Recent breakthroughs in LMMs have significantly enhanced visual understanding capabilities, leading to growing popularity and widespread application across various domains [19, 24, 35, 56, 57, 60, 62]. Inspired by DeepSeek-R1 [11], many of these methods leverage reinforcement learning (RL) with reward engineering to shape effective thinking processes and solve increasingly complex reasoning tasks [13, 31, 44, 46, 49, 55, 59, 60]. Despite recent progress, most LMMs still struggle with high-resolution image inputs and typically impose a resolution constraint due to limited visual-token capacity [12, 23, 26, 28]. This can result in blurred images and loss of key visual information, resulting in performance degradation. Such limitations further restrict the application of LMMs in high-resolution real-world scenarios, such as remote sensing and autonomous driving [8]. While recent works [6, 14, 40, 61] attempt to address this issue, they often require more thinking time and higher training costs. In contrast, our work adopts a visual grounded reasoning process to address the challenges posed by high-resolution image analysis.

2.2. Visual Grounded Reasoning Models

Visual grounding LMMs aim to predict and focus on the key ROIs before actually answering the question [52]. Existing studies highlight that this process is similar to human visual

processing and can ensure more accurate answers through grounded reasoning [27, 30, 58, 64]. There are two lines of work that study the optimization of visual grounding capabilities. One direction focuses on directly fine-tuning models on labeled data that contain ground-truth bounding box annotations of key image regions [32, 37, 39]. The differences between the predicted and ground-truth bounding boxes are used to update the policies. For example, Wang et al. [48] introduce the TreeBench dataset, whose region labels are manually curated by eight human experts. Based on this dataset, they explicitly supervised the model’s bounding box prediction for each training instance and reported high grounding accuracy throughout the high-resolution visual understanding process. While such approaches can directly optimize the grounding capabilities of LMMs, they require large-scale and costly manual annotations [22].

Another line of research seeks to leverage end-to-end RL to improve grounding capabilities without external visual annotations [16, 41, 65]. However, these RL-based approaches typically post-train the model leveraging a reward signal derived from only the correctness of the final answer [48]. Consequently, they do not directly optimize grounding performance. We observed that annotation-free methods that directly optimize grounding capabilities remain undiscovered, as it is challenging to assess the grounding accuracy without bounding box annotations. Leveraging visual feedback, we aim to directly optimize the grounding capability of LMMs. Therefore, our work provides a more flexible solution that enables the model to self-verify its localization results for policy updates.

3. Preliminaries

3.1. Grounding-Based Visual Reasoning

Visual grounding refers to the task of localizing visual elements in an image based on a linguistic question. Grounding capabilities enable existing models to focus on critical visual regions that correspond to the given linguistic concepts, thereby effectively reducing redundant computations in high-resolution vision-centric tasks [27, 64]. Formally, given an input image I_f and a textual question q , the visual grounding model first identifies the key sub-images I_s that semantically align with the entities or relations described in q , denoted as $I_s \sim \pi_\theta(\cdot | I_f, q)$, where π_θ denotes the model policy parameterized by θ . Next, the model leverages the task-relevant regions and generates an answer a based on both the full image and key sub-images, that is, $a \sim \pi_\theta(\cdot | I_f, I_s, q)$.

3.2. Group Relative Policy Optimization

Group Relative Policy Optimization (GRPO) [38] is an efficient and effective RL algorithm for post-training. For a question-answer pair, GRPO first generates a group of G

Table 1. The proportion of incorrect grounding and correct grounding for Qwen2.5-VL-7B [3] and InternVL3-8B [66] on the TreeBench dataset [48]. The IoU threshold is set to 0.3.

Method	Incorrect Grounding		Correct Grounding	
	Count/Total	Proportion	Count/Total	Proportion
Qwen2.5-VL-7B [3]	192 / 334	57.5%	142 / 334	42.5%
InternVL3-8B [66]	305 / 305	90.0%	34 / 305	10.0%

candidate responses $\{o_i\}_{i=1}^G$ and receives corresponding rewards $\{r_i\}_{i=1}^G$. The advantage A_i of each response is computed in a group-relative manner:

$$A_i = \frac{r_i - \text{mean}(\{r_i\}_{i=1}^G)}{\text{std}(\{r_i\}_{i=1}^G)}, \quad (1)$$

where $\text{mean}(\cdot)$ and $\text{std}(\cdot)$ are the mean and standard deviation of the rewards. The policy π_θ is updated as follows:

$$\mathcal{J}_{\text{GRPO}}(\theta) = \frac{1}{G} \sum_{i=1}^G \left(\frac{\pi_\theta(o_i|q)}{\pi_{\theta_{\text{old}}}(o_i|q)} A_i - \beta \mathbb{D}_{\text{KL}}(\pi_\theta \| \pi_{\text{ref}}) \right), \quad (2)$$

where β balances the KL-penalty term, $\pi_{\theta_{\text{old}}}$ is the old model, and π_{ref} is the reference model.

4. The Proposed Method

In this section, we begin with pilot experiments designed to illustrate the challenges faced by annotation-free visual grounding methods, which serve as the research foundation for our study. Then, we introduce the idea of our approach HART, a closed-loop framework that directly optimizes grounding and reasoning without relying on additional annotated data.

4.1. Vanishing Advantages in Indirect Optimization

The rewards of annotation-free visual grounding methods measure the correctness of the final answer but cannot directly reflect grounding accuracy. As a result, they receive a positive reward when the final answer is correct even though the grounding is incorrect, as illustrated in Figure 2(a). While this phenomenon is theoretically possible, its real-world occurrence and frequency remain unclear. Therefore, we conduct pilot experiments on LMMs grounding and reasoning, taking Qwen2.5-VL-7B [3] and InternVL3-8B [66] as representative examples. Specifically, we analyze grounding accuracy when the final answer is correct.

Experimental settings. Both models are evaluated on the TreeBench dataset [48], since it provides ground-truth bounding box annotations of key image regions relevant to the questions. TreeBench contains a series of high-resolution visual tasks, categorized into perception and reasoning domains. Its average resolution is $2,152 \times 1,615$. We adopt Intersection over Union (IoU) as the metric to

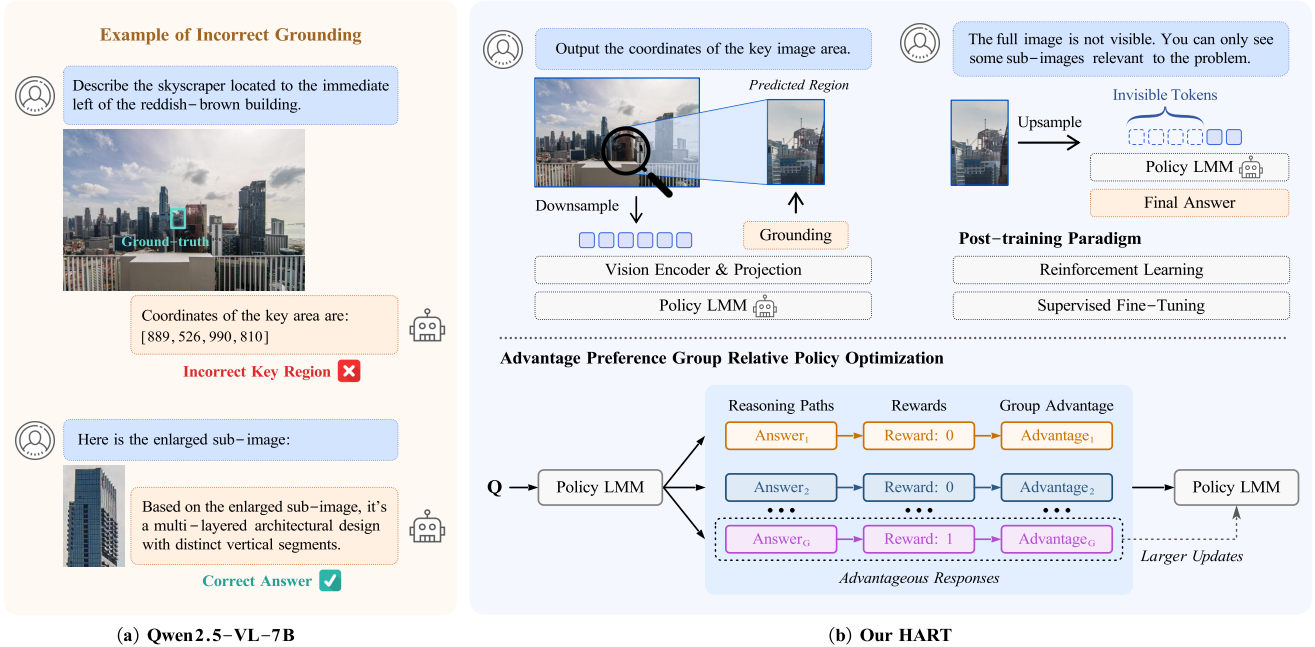


Figure 2. Left: An example of Qwen-2.5-VL-7B where the final answer is correct but the grounding is incorrect. Right: **HART Framework**. The post-training strategy consists of Reinforcement Learning (RL) and Supervised Fine-Tuning (SFT). In stage 1, after identifying the ROIs, the model answers based solely on the sub-regions and the original question. AP-GRPO is introduced to improve the model’s grounding capabilities. In stage 2, HART uses SFT to further enhance the high-resolution reasoning capabilities.

evaluate grounding accuracy under the condition that the final answer is correct. Specifically, grounding is considered correct if at least one predicted bounding box has an IoU greater than 0.3 with the ground-truth box.

Experimental results. As demonstrated in Table 1, Qwen-2.5-VL-7B correctly answers 163 questions on TreeBench, containing a total of 334 ground-truth bounding boxes, among which only 42.5% are correctly localized. Another popular model, InternVL3-8B, correctly answers 171 questions, containing a total of 339 ground-truth bounding boxes. Its grounding accuracy is only 10.0%.

Existing annotation-free visual grounding methods typically post-train LMMs using only the final answer as the training signal [16, 65]. Based on our pilot experiments, we identify two limitations of these methods. First, it becomes difficult to quantify the actual contribution of the grounding. Second, in more than half of the cases where the models receive a positive reward, the localization is incorrect. Such reward misspecification can lead to negative optimization of grounding performance, as the model policy tends to encourage unreliable reasoning process. These limitations further restrict performance on visually intensive tasks.

4.2. HART

To overcome the above limitations, a novel closed-loop framework named *High-resolution Annotation-free Reasoning Technique (HART)* is proposed to directly op-

imize high-resolution visual grounding and understanding. As illustrated in Figure 2(b), we extend the idea of decomposing the reasoning process from current research [22] to visual grounding LMMs. We also take into account the maximum-token constraint adopted in many models and therefore restrict image resolution in the first turn.

During the training phase, our proposed HART first prompts the model to predict the key ROIs conditioned on the down-sampled full input image I_f and the textual question q . The instruction is: *Output the coordinates of the key image area relevant to the problem $[I_f, q]$* . The model’s response is returned in bounding-box format. In the second step, HART assesses whether the visual grounding is sufficient for generating the final answer. The ROIs I_s are cropped from the original high-resolution image, and then the original image is deliberately withheld. The next instruction is adjusted based on the visual feedback: *You were supposed to answer a question based on a full image, but now the full image is not visible. You can only see some sub-regions $[I_s]$ relevant to the problem. Answer the following question: $[q]$* . If the model can answer this instruction correctly based on the sub-regions, we consider that these regions contain all the visual information needed to answer the question, indicating a faithful grounding.

Let $L \in \{0, 1\}$ denote whether the model localizes the correct region and $R \in \{0, 1\}$ denote whether it produces the correct response. Compared to baseline pipelines, the

Table 2. Answer accuracy of state-of-the-art models on the in-distribution dataset MME-RealWorld-Lite [63]. Bold numbers are the best results. Abbreviations: RS-Remote Sensing; MO-Monitoring; DT-Diagram and Table; AD-Autonomous Driving; OCR-Optical Character Recognition in the Wild.

Method	Parameters	Perception					Reasoning				Overall
		RS	MO	AD	DT	OCR	MO	AD	DT	OCR	
<i>Open-source General Models</i>											
Qwen2.5-VL-7B [3]	7B	32.7	27.3	30.0	83.0	87.6	28.7	23.0	62.0	72.0	42.3
LLaVA-OneVision-7B [20]	7B	40.0	31.7	39.4	56.0	80.0	38.0	32.0	33.0	65.0	43.7
InternVL3-8B [66]	8B	49.3	34.5	36.9	75.0	83.6	40.0	37.0	44.0	70.0	47.9
<i>Visual Grounded Reasoning Models</i>											
Pixel-Reasoner-7B [41]	7B	52.0	38.9	30.9	86.0	89.6	46.0	32.5	72.0	71.0	49.7
DeepEyes-7B [65]	7B	52.7	43.3	33.4	89.0	90.0	44.0	35.0	69.0	76.0	53.2
<i>Qwen2.5-VL-7B with Post-Training</i>											
SFT	7B	48.0	48.6	45.4	87.0	90.8	56.7	35.5	71.0	73.0	55.8
GRPO [38]	7B	38.7	41.7	32.3	82.0	89.2	46.7	38.3	70.0	75.0	50.9
MGPO [16]	7B	54.0	46.7	44.0	78.0	86.4	52.7	39.3	69.0	74.0	60.5
HART-7B (Ours)	7B	58.7	49.8	57.7	86.0	89.6	58.7	51.0	75.0	72.0	62.4
<i>Larger-scale Open-source Models</i>											
Qwen2.5-VL-32B [3]	32B	40.7	29.5	40.7	83.0	87.2	27.3	29.5	60.0	74.0	45.6
InternVL3-38B [66]	38B	56.0	42.6	40.0	71.0	85.6	47.3	35.0	45.0	77.0	51.0
Qwen2.5-VL-72B [3]	72B	34.0	27.9	30.6	87.0	90.8	26.7	25.5	61.0	74.0	43.7
LLaVA-OneVision-72B [20]	72B	50.7	37.9	40.0	67.0	79.2	38.7	39.3	41.0	76.0	48.7
<i>Private Models</i>											
GPT-4o-mini [33]	—	6.7	26.5	24.2	44.2	62.5	25.8	26.8	39.1	47.0	36.4
Gemini-1.5-Pro [45]	—	14.0	31.1	26.6	39.9	67.6	28.3	19.2	33.2	52.7	38.2
GPT-4o [17]	—	28.9	33.9	22.4	46.7	77.7	36.5	26.4	44.8	61.4	45.2
Claude 3.5 Sonnet [1]	—	25.7	32.2	40.8	67.4	72.5	41.8	31.9	61.2	61.9	51.6

probability of our model producing a correct answer while localizing the incorrect region is much closer to zero, leading to a lower entropy. We state our result as follows.

Proposition 1 Let $I_{HART}(L; R)$ and $I_{baseline}(L; R)$ denote the mutual information between localization correctness L and response correctness R under our method and baselines, respectively. Then,

$$I_{HART}(L; R) > I_{baseline}(L; R). \quad (3)$$

We prove this proposition in Appendix A. The above expression shows that HART strengthens causal dependency between localization and reasoning. The feedback loop offers two benefits: (a) It enables the model to self-verify its localization results, eliminating the need for manual bounding box annotations. (b) The model can access more detailed visual information as we zoom in on the key region of the original image. This design reduces redundant computations and overcomes maximum pixel constraints imposed by existing LMMs, thereby enhancing the effectiveness in high-resolution real-world scenarios.

4.3. Advantage Preference Policy Optimization

We propose a post-training strategy to further improve the model’s grounding and reasoning capabilities. In the HART framework, a correct final response indicates that the localized ROIs contain all the visual information needed to answer the question. Hence, rewarding correct answers also fosters faithful grounding. Motivated by this observation,

we proceed to modify the standard GRPO algorithm [38] to optimize the localization policy.

In vanilla GRPO, all samples are assigned equal weight. However, samples with incorrect responses clearly exhibit higher localization uncertainty, which can lead to reward misspecification within our feedback loop. Therefore, different from the traditional post-training methods, we prefer correct and advantageous responses as they indicate faithful grounding. Accordingly, we propose *Advantage Preference Group Relative Policy Optimization (AP-GRPO)* to assign dynamic weights to responses based on their advantages, thus allowing the model to focus more on optimizing the samples with correct grounding. In particular, given a textual question and the cropped sub-images, AP-GRPO first generates a group of candidate responses and receives corresponding rewards $\{r_i\}_{i=1}^G$, where $r_i = 1$ indicates a correct answer and $r_i = 0$ indicates an incorrect answer. Then the advantages of each response are computed, and the optimization objective is as follows:

$$\mathcal{J}_{AP-GRPO}(\theta) = \frac{1}{G} \sum_{i=1}^G (\mu_1 \frac{\pi_{\theta}(o_i|q)}{\pi_{\theta_{old}}(o_i|q)} A_i - \mu_2 \mathbb{D}_{KL}(\pi_{\theta} || \pi_{ref})), \quad (4)$$

$$\mu_1 = 1 + k(r_i - \text{mean}(\{r_i\}_{i=1}^G)), \quad (5)$$

$$\mu_2 = \beta \left(1 - k(r_i - \text{mean}(\{r_i\}_{i=1}^G)) \right), \quad (6)$$

where the scaling factor k is the only hyperparameter in HART. First, the samples with correct grounding are assigned higher weights with the parameter μ_1 , which provides larger updates for advantageous responses. Next, we

Table 3. Answer accuracy of state-of-the-art models on the out-of-distribution dataset TreeBench [48]. Bold numbers are the best results.

Method	Parameters	Attributes	OCR	Phy. State	Obj. Retr.	Material	Comparison	Ordering	Con. & Oc.	Spa. Cont.	Per. Trans.	Overall
		Perception					Reasoning					
<i>Open-source General Models</i>												
Qwen2.5-VL-7B [3]	7B	55.2	27.9	56.5	62.5	53.8	43.2	35.1	39.0	44.8	20.0	37.0
LLaVA-OneVision-7B [20]	7B	55.2	32.4	56.5	50.0	53.8	36.4	22.8	41.5	72.4	21.2	37.3
InternVL3-8B [66]	8B	51.7	33.7	56.5	56.3	69.2	43.2	24.6	39.0	72.4	21.2	38.8
<i>Visual Grounded Reasoning Models</i>												
DeepEyes-7B [65]	7B	62.1	51.5	65.2	68.8	53.8	47.7	24.6	36.6	51.7	11.8	37.5
Pixel-Reasoner-7B [41]	7B	58.6	48.5	65.2	50.0	61.5	40.9	31.6	39.0	44.8	14.1	39.0
<i>Qwen2.5-VL-7B with Post-Training</i>												
SFT	7B	62.1	50.0	52.2	62.5	61.5	45.5	24.6	43.9	48.3	16.5	40.0
GRPO [38]	7B	48.3	48.5	65.2	56.3	53.9	50.0	28.1	43.9	48.3	14.1	39.5
MGPO [16]	7B	51.7	48.5	56.5	68.8	61.5	43.2	35.1	43.9	44.8	11.8	39.5
HART-7B (Ours)	7B	62.1	55.9	52.2	56.3	61.5	50.0	35.1	48.8	62.1	14.1	43.7
<i>Larger-scale Open-source Models</i>												
Qwen2.5-VL-32B [3]	32B	51.7	54.4	69.6	62.5	53.8	38.6	33.3	46.3	62.1	16.5	42.5
InternVL3-38B [66]	38B	51.7	51.5	52.2	68.8	61.5	38.6	33.3	56.1	65.5	12.9	42.0
Qwen2.5-VL-72B [3]	72B	65.5	48.5	56.5	56.3	69.2	38.6	33.3	51.2	72.4	11.8	42.2
LLaVA-OneVision-72B [20]	72B	62.1	36.8	65.2	62.3	53.8	47.7	28.1	53.7	65.5	12.9	40.5
<i>Private Models</i>												
Gemini-2.5-Flash [9]	—	48.3	75.0	69.6	68.8	53.9	43.2	19.3	56.1	72.4	15.3	45.9
GPT-4o [17]	—	51.7	69.1	65.2	43.8	61.5	43.2	38.6	48.8	72.4	18.8	46.9
Gemini-2.5-Pro [10]	—	51.7	83.8	56.5	75.0	61.5	54.6	36.8	65.9	86.2	20.0	54.1
o3 [34]	—	69.0	79.4	65.2	68.8	69.2	50.0	38.6	61.0	86.2	22.4	54.8

introduce a dynamic weighting for the KL penalty coefficient. The dynamic weight factor μ_2 reduces the KL penalty when the grounding is correct, thereby allowing greater deviation from the reference model.

Theoretical guarantees of AP-GRPO. To theoretically understand the advantages of the proposed AP-GRPO in comparison to prior studies, the following proposition verifies that AP-GRPO reduces reward misspecification that typically causes negative optimization of grounding performance. The proof is provided in Appendix B.

Proposition 2 Let $g_{AP-GRPO}$ and $g_{baseline}$ denote the gradients of AP-GRPO and baselines, respectively. Consider any single-step reinforcement learning environment with binary rewards. Then,

$$g_{AP-GRPO} = g_{baseline} - P(L = 0, r = 1) \mathbb{E}_{L=0, r=1} [\nabla_{\theta} \log \pi_{\theta}]. \quad (7)$$

In other words, Proposition 2 demonstrates that AP-GRPO effectively reduces the negative impact of reward misspecification seen in prior studies. As shown by Eq. (7), AP-GRPO utilizes the subset of samples where both grounding and reasoning are correct, providing a conservative approximation of the ground-truth gradient. Consequently, answer correctness becomes a more accurate reflection of perception quality, which forms the theoretical foundation of the proposed AP-GRPO. Compared with vanilla GRPO, which assigns equal weight to all samples, AP-GRPO has several

significant advantages: (a) It enhances visual understanding and feature extraction by encouraging attention to the correct ROIs within the image. (b) The model’s grounding capabilities are directly optimized without relying on additional visual supervision, since AP-GRPO allows the reward signal to evaluate the grounding performance. (c) The proposed strategy also ensures interpretable reasoning.

Although AP-GRPO enables the model to learn precise visual localization, withholding full visual information inevitably causes a decrease in answer accuracy. Building upon the RL strategy, we further apply SFT to enhance the model’s high-resolution reasoning capabilities. In the SFT phase, the original image is fully visible to the model. Following [5], we adopt a clean dataset separation: \mathcal{D}_{SFT} for SFT and \mathcal{D}_{RL} for RL. The loss function is represented as

$$\mathcal{L}(\theta) = -\mathbb{E}_{(x,y) \sim \mathcal{D}_{SFT}} \sum_{i=1}^T \log P(y_i | x, y_{<i}); \quad (8)$$

where T is the text length and (x, y) represents the query and target response in dataset \mathcal{D}_{SFT} .

5. Experiments

5.1. Experimental Settings

Benchmarks. We evaluate the proposed method on several benchmarks targeting high-resolution visual understanding capabilities of LMMs. (a) The MME-RealWorld dataset [63] comprises challenging visual

Table 4. Answer accuracy on other multimodal benchmarks.

Benchmark	Resolution	Qwen2.5-VL-7B [3]	HART-7B (Ours)
MMStar [4]	511 × 391	59.3	62.8
V* Bench [53]	2, 246 × 1, 583	78.5	80.6
HR-Bench-4K [51]	4, 023 × 3, 503	70.1	71.1
HR-Bench-8K [51]	5, 727 × 4, 430	61.0	71.9

Table 5. Grounding performance of HART and baselines on the out-of-distribution dataset TreeBench [48]. Bold numbers are the best results. The IoU threshold is set to 0.3.

Method	Incorrect Grounding		Correct Grounding	
	Count	Proportion	Count	Proportion
Qwen2.5-VL-7B [3]	522	62.7%	311	37.3%
LLaVA-OneVision-7B [20]	726	87.2%	107	12.9%
InternVL3-8B [66]	750	90.0%	83	10.0%
<i>Qwen2.5-VL-7B with Post-Training</i>				
SFT	558	67.0%	275	33.0%
GRPO [38]	506	60.7%	327	39.3%
MGPO [16]	488	58.6%	345	41.4%
HART-7B (Ours)	442	53.1%	391	46.9%

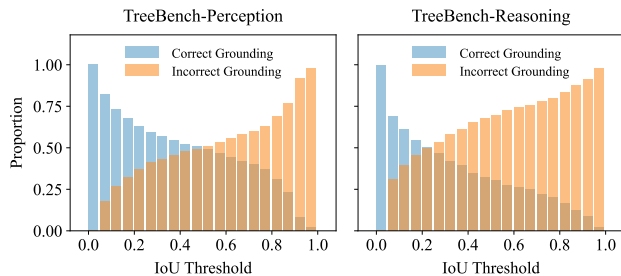


Figure 3. Grounding performance of HART on TreeBench-Perception and TreeBench-Reasoning.

question-answering pairs, with an average resolution of $2,076 \times 1,434$. We use its training set for post-training, randomly sampling 10K examples for \mathcal{D}_{RL} and assigning the remainder to \mathcal{D}_{SFT} . Its test set, also referred to as MME-RealWorld-Lite, contains 1,919 samples and is used for in-distribution evaluation. (b) TreeBench [48] serves as an out-of-distribution benchmark with an average image resolution of $2,152 \times 1,615$. Specifically, TreeBench contains a total of 833 manually annotated bounding boxes, providing a basis for evaluating grounding capabilities. Each sample in the datasets follows a multiple-choice format. The evaluation metric is the multiple-choice accuracy.

Baselines. We compare HART with several state-of-the-art baselines. (a) Private models including GPT-4o [17], Gemini series [9], etc.. (b) Open-source general models including Qwen2.5-VL series [3], LLaVA-OneVision series [20], and InternVL3 series [66]. (c) Representative visual grounded reasoning models including Pixel-Reasoner [41] and DeepEyes [65]. (d) Post-training methods including SFT, GRPO [38], and the recently proposed

Table 6. Ablations of each component of our HART.

Method	k	MME-RealWorld-Lite		TreeBench	
		Perception	Reasoning	Perception	Reasoning
Qwen2.5-VL-7B [3]	-	46.4	35.9	43.6	33.2
<i>+ Post-Training</i>					
SFT	-	59.9	49.5	55.0	31.2
GRPO [38]	-	52.1	49.1	52.3	32.0
HART-7B (Ours)					
· GRPO w/ SFT	0.00	63.8	52.7	51.7	34.0
· AP-GRPO	0.15	51.2	47.5	51.0	32.4
· AP-GRPO w/ SFT	0.15	67.0	56.9	56.4	31.6
· AP-GRPO	0.30	53.6	49.9	55.0	33.6
· AP-GRPO w/ SFT	0.30	64.1	56.0	57.7	34.8
· AP-GRPO	0.60	53.3	48.0	52.3	33.6
· AP-GRPO w/ SFT	0.60	64.9	58.5	57.0	35.9

MGPO [16] for high-resolution vision-centric tasks.

Implementation Details. We employ the Transformer Reinforcement Learning (TRL) framework [47] to enable distributed training and use Qwen2.5-VL-7B [3] as the base model. Both GRPO and AP-GRPO employ a binary reward function that evaluates answer correctness. The hyperparameter k in AP-GRPO is set to 0.6. More training details are provided in Appendix C.

5.2. Main Results

We evaluate the answer accuracy of our proposed method HART on popular high-resolution visual benchmarks. Table 2 presents the accuracy comparison between HART and baselines on the in-distribution dataset. HART achieves an accuracy of 62.4% on MME-RealWorld-Lite, surpassing even Qwen2.5-VL-72B and LLaVA-OneVision-72B, both of which have much larger parameters. Notably, our HART outperforms the representative private and open-source models in most perception and reasoning tasks. Compared to the base model Qwen2.5-VL-7B [3], the proposed method achieves remarkable improvements on challenging tasks, *i.e.*, +26.0% on Remote Sensing, +27.7% on Perception-Autonomous Driving, and +30.0% on Reasoning-Monitoring tasks, indicating enhanced fine-grained visual understanding. We can observe that visual grounding methods are able to improve the model’s performance on high-resolution visual tasks. Among them, HART achieves the highest average accuracy, demonstrating the effectiveness of our closed-loop framework.

Next, we evaluate the models on out-of-distribution datasets. As shown in Table 3, our HART also achieves open-source state-of-the-art on TreeBench with an accuracy of 43.7%. HART delivers significant improvements over the base model Qwen2.5-VL-7B, surpassing other post-training paradigms such as SFT and GRPO. This demonstrates the effectiveness of the proposed post-training strategy in improving the joint understanding of visual and textual inputs. In Table 4, we further compare HART with the base model Qwen2.5-VL-7B on a range of multimodal bench-

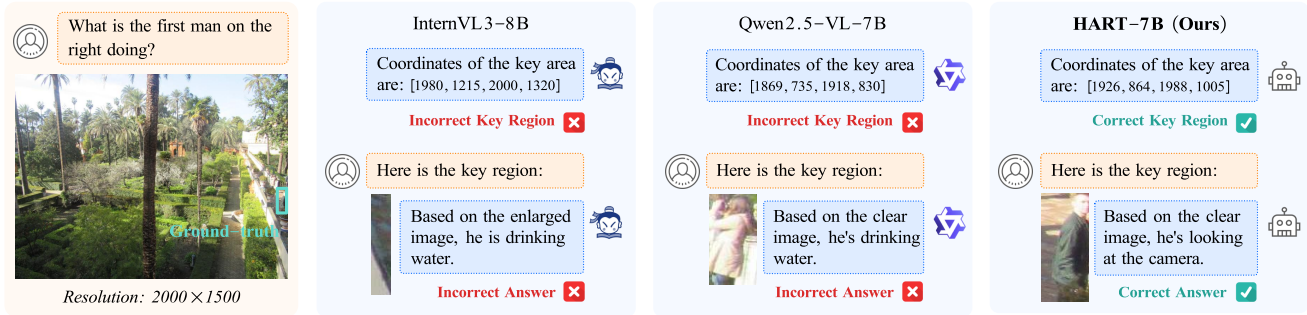


Figure 4. Visualization of model outputs from InternVL3-8B [66], Qwen2.5-VL-7B [3], and our method HART-7B on TreeBench [48].

marks covering both low- and high-resolution visual tasks. Detailed results are provided in Appendix D. The results highlight the strong adaptability of our method across visual scenes of different resolutions. In conclusion, our HART provides a flexible solution that adapts better to high-resolution real-world scenarios.

5.3. Grounding Results

In this section, we evaluate the grounding accuracy of the proposed method on high-resolution visual tasks. We utilize IoU as the metric to measure grounding accuracy. Table 5 presents the grounding performance with an IoU threshold of 0.3. HART achieves superior grounding capabilities, outperforming the second-best result by 5.5%, indicating its effectiveness in accurately localizing key regions. While both HART and MGPO adopt a visual grounded reasoning pipeline for post-training, the issue of reward misspecification limits MGPO’s ability to deliver substantial improvements over the base model Qwen2.5-VL-7B. In contrast, HART can self-verify its localization results for policy updates, leading to more accurate localization. Additionally, we report HART’s grounding performance over a range of IOU thresholds (0.0 to 0.95) in Figure 3. These results suggest that HART offers an effective optimization strategy for enhancing both grounding and reasoning capabilities.

5.4. Ablation Studies

In this experiment, we first conduct ablation studies to investigate the influence of each component of HART. As demonstrated in Table 6, we compare the answer accuracy of post-trained Qwen2.5-VL-7B [3] with vanilla GRPO, vanilla SFT, and the proposed HART on MME-RealWorld-Lite [63] and TreeBench [48], respectively. The results indicate that both RL (Stage 1) and SFT (Stage 2) are crucial for enhancing visual understanding, as HART yields considerably higher accuracy than either stage alone. In the table we also present the results of the sensitivity analysis on hyperparameter k , varying it in $\{0.00, 0.15, 0.30, 0.60\}$. HART consistently improves performance under different values of k , demonstrating its robustness. Detailed results

are shown in Appendix D.

5.5. Visualization Results

We present a visualized comparison of our method against prior methods in Figure 4. In this example, the task requires attending to the right-most man before executing the reasoning step. Compared with InternVL3-7B [66] and Qwen2.5-VL-7B [3], our method identifies the critical region more reliably and achieves a more accurate reasoning outcome. More visualization results are shown in Appendix E.

6. Conclusion

This paper proposes HART, a closed-loop framework designed for high-resolution visual tasks. HART enables LMMs to identify and self-verify key regions of interest conditioned on visual and textual inputs. To guide its localization behavior, we propose AP-GRPO to prioritize optimizing samples with correct grounding behavior, without relying on external visual supervision. Empirical results demonstrate enhanced visual understanding across multiple high-resolution vision-centric tasks. In summary, HART provides a foundation for further exploration in the joint optimization of grounding and reasoning capabilities.

Future works. This work focuses on optimizing a 7B-parameter base model. Future research will focus on scaling up training datasets and model size for further improvements. Additionally, accelerating the visual grounded reasoning process needs comprehensive investigation.

References

- [1] Anthropic. Claude 3.5 sonnet. <https://www.anthropic.com/news/claude-3-5-sonnet>, 2024. 5
- [2] Kazi Hasan Ibn Arif, JinYi Yoon, Dimitrios S Nikolopoulos, Hans Vandierendonck, Deepu John, and Bo Ji. Hired: Attention-guided token dropping for efficient inference of high-resolution vision-language models. In *Proceedings of the AAAI Conference on Artificial Intelligence*, pages 1773–1781, 2025. 1

- [3] Shuai Bai, Keqin Chen, Xuejing Liu, Jialin Wang, Wenbin Ge, Sibao Song, Kai Dang, Peng Wang, Shijie Wang, Jun Tang, et al. Qwen2. 5-vl technical report. *arXiv preprint arXiv:2502.13923*, 2025. 1, 2, 3, 5, 6, 7, 8
- [4] Lin Chen, Jinsong Li, Xiaoyi Dong, Pan Zhang, Yuhang Zang, Zehui Chen, Haodong Duan, Jiaqi Wang, Yu Qiao, Dahua Lin, et al. Are we on the right way for evaluating large vision-language models? *Advances in Neural Information Processing Systems*, 37:27056–27087, 2024. 7
- [5] Liang Chen, Xueting Han, Li Shen, Jing Bai, and Kam-Fai Wong. Beyond two-stage training: Cooperative sft and rl for llm reasoning. *arXiv preprint arXiv:2509.06948*, 2025. 6
- [6] Zhe Chen, Weiyun Wang, Hao Tian, Shenglong Ye, Zhangwei Gao, Erfei Cui, Wenwen Tong, Kongzhi Hu, Jiapeng Luo, Zheng Ma, et al. How far are we to gpt-4v? closing the gap to commercial multimodal models with open-source suites. *Science China Information Sciences*, 67(12):220101, 2024. 2
- [7] Yunkai Dang, Kaichen Huang, Jiahao Huo, Yibo Yan, Sirui Huang, Dongrui Liu, Mengxi Gao, Jie Zhang, Chen Qian, Kun Wang, et al. Explainable and interpretable multimodal large language models: A comprehensive survey. *arXiv preprint arXiv:2412.02104*, 2024. 1
- [8] Xiaoyi Dong, Pan Zhang, Yuhang Zang, Yuhang Cao, Bin Wang, Linke Ouyang, Songyang Zhang, Haodong Duan, Wenwei Zhang, Yining Li, et al. Internlm-xcomposer2-4khd: A pioneering large vision-language model handling resolutions from 336 pixels to 4k hd. *Advances in Neural Information Processing Systems*, 37:42566–42592, 2024. 1, 2
- [9] Google DeepMind. Gemini-2.5-flash. <https://deepmind.google/models/gemini/flash/>, 2025. 6, 7
- [10] Google DeepMind. Gemini-2.5-pro. <https://deepmind.google/models/gemini/pro/>, 2025. 1, 6
- [11] Daya Guo, Dejian Yang, Haowei Zhang, Junxiao Song, Peiyi Wang, Qihao Zhu, Runxin Xu, Ruoyu Zhang, Shirong Ma, Xiao Bi, et al. Deepseek-r1 incentivizes reasoning in llms through reinforcement learning. *Nature*, 645(8081):633–638, 2025. 1, 2
- [12] Zonghao Guo, Ruyi Xu, Yuan Yao, Junbo Cui, Zanlin Ni, Chunjiang Ge, Tat-Seng Chua, Zhiyuan Liu, and Gao Huang. Llava-uhd: an lmm perceiving any aspect ratio and high-resolution images. In *European Conference on Computer Vision*, pages 390–406. Springer, 2024. 2
- [13] Zirun Guo, Minjie Hong, and Tao Jin. Observe-r1: Unlocking reasoning abilities of mllms with dynamic progressive reinforcement learning. *arXiv preprint arXiv:2505.12432*, 2025. 2
- [14] Anwen Hu, Haiyang Xu, Jiabo Ye, Ming Yan, Liang Zhang, Bo Zhang, Chen Li, Ji Zhang, Qin Jin, Fei Huang, and Jingren Zhou. mplug-docowl 1.5: Unified structure learning for ocr-free document understanding. *CoRR*, abs/2403.12895, 2024. 2
- [15] Runhui Huang, Xinpeng Ding, Chunwei Wang, Jianhua Han, Yulong Liu, Hengshuang Zhao, Hang Xu, Lu Hou, Wei Zhang, and Xiaodan Liang. Hires-llava: Restoring fragmentation input in high-resolution large vision-language models. In *Proceedings of the Computer Vision and Pattern Recognition Conference*, pages 29814–29824, 2025. 1
- [16] Xinyu Huang, Yuhao Dong, Weiwei Tian, Bo Li, Rui Feng, and Ziwei Liu. High-resolution visual reasoning via multi-turn grounding-based reinforcement learning. *arXiv preprint arXiv:2507.05920*, 2025. 2, 3, 4, 5, 6, 7
- [17] Aaron Hurst, Adam Lerer, Adam P Goucher, Adam Perelman, Aditya Ramesh, Aidan Clark, AJ Ostrow, Akila Welihinda, Alan Hayes, Alec Radford, et al. Gpt-4o system card. *arXiv preprint arXiv:2410.21276*, 2024. 1, 5, 6, 7
- [18] Aaron Jaech, Adam Kalai, Adam Lerer, Adam Richardson, Ahmed El-Kishky, Aiden Low, Alec Helyar, Aleksander Madry, Alex Beutel, Alex Carney, et al. Openai o1 system card. *arXiv preprint arXiv:2412.16720*, 2024. 1
- [19] Bo Li, Yuanhan Zhang, Dong Guo, Renrui Zhang, Feng Li, Hao Zhang, Kaichen Zhang, Yanwei Li, Ziwei Liu, and Chunyuan Li. Llava-onevision: Easy visual task transfer. *CoRR*, abs/2408.03326, 2024. 2
- [20] Bo Li, Yuanhan Zhang, Dong Guo, Renrui Zhang, Feng Li, Hao Zhang, Kaichen Zhang, Peiyuan Zhang, Yanwei Li, Ziwei Liu, et al. Llava-onevision: Easy visual task transfer. *arXiv preprint arXiv:2408.03326*, 2024. 2, 5, 6, 7
- [21] Zhang Li, Biao Yang, Qiang Liu, Zhiyin Ma, Shuo Zhang, Jingxu Yang, Yabo Sun, Yuliang Liu, and Xiang Bai. Monkey: Image resolution and text label are important things for large multi-modal models. In *proceedings of the IEEE/CVF conference on computer vision and pattern recognition*, pages 26763–26773, 2024. 1
- [22] Zongxia Li, Wenhao Yu, Chengsong Huang, Rui Liu, Zhenwen Liang, Fuxiao Liu, Jingxi Che, Dian Yu, Jordan Boyd-Graber, Haitao Mi, et al. Self-rewarding vision-language model via reasoning decomposition. *arXiv preprint arXiv:2508.19652*, 2025. 3, 4
- [23] Chaohu Liu, Kun Yin, Haoyu Cao, Xinghua Jiang, Xin Li, Yinsong Liu, Deqiang Jiang, Xing Sun, and Linli Xu. Hrvda: High-resolution visual document assistant. In *Proceedings of the IEEE/CVF conference on computer vision and pattern recognition*, pages 15534–15545, 2024. 2
- [24] Haotian Liu, Chunyuan Li, Yuheng Li, and Yong Jae Lee. Improved baselines with visual instruction tuning. In *Proceedings of the IEEE/CVF conference on computer vision and pattern recognition*, pages 26296–26306, 2024. 2
- [25] Shilong Liu, Hao Cheng, Haotian Liu, Hao Zhang, Feng Li, Tianhe Ren, Xueyan Zou, Jianwei Yang, Hang Su, Jun Zhu, et al. Llava-plus: Learning to use tools for creating multimodal agents. In *European conference on computer vision*, pages 126–142. Springer, 2024. 1
- [26] Yuliang Liu, Biao Yang, Qiang Liu, Zhang Li, Zhiyin Ma, Shuo Zhang, and Xiang Bai. Textmonkey: An ocr-free large multimodal model for understanding document. *CoRR*, abs/2403.04473, 2024. 2
- [27] Zuyan Liu, Yuhao Dong, Yongming Rao, Jie Zhou, and Jiwen Lu. Chain-of-spot: Interactive reasoning improves large vision-language models. *CoRR*, abs/2403.12966, 2024. 1, 3
- [28] Zuyan Liu, Yuhao Dong, Ziwei Liu, Winston Hu, Jiwen Lu, and Yongming Rao. Oryx MLLM: On-demand spatial-temporal understanding at arbitrary resolution. In *The Thir-*

- teenth International Conference on Learning Representations*, 2025. 1, 2
- [29] Ziyu Liu, Zeyi Sun, Yuhang Zang, Xiaoyi Dong, Yuhang Cao, Haodong Duan, Dahua Lin, and Jiaqi Wang. Visual-rl: Visual reinforcement fine-tuning. *arXiv preprint arXiv:2503.01785*, 2025. 1
- [30] Bozhi Luan, Hao Feng, Hong Chen, Yonghui Wang, Wengang Zhou, and Houqiang Li. Textcot: Zoom in for enhanced multimodal text-rich image understanding. *CoRR*, abs/2404.09797, 2024. 2, 3
- [31] Fanqing Meng, Lingxiao Du, Zongkai Liu, Zhixiang Zhou, Quanfeng Lu, Daocheng Fu, Tiancheng Han, Botian Shi, Wenhai Wang, Junjun He, et al. Mm-eureka: Exploring the frontiers of multimodal reasoning with rule-based reinforcement learning. *arXiv preprint arXiv:2503.07365*, 2025. 2
- [32] Minheng Ni, Zhengyuan Yang, Linjie Li, Chung-Ching Lin, Kevin Lin, Wangmeng Zuo, and Lijuan Wang. Point-rl: Improving multimodal reasoning with visually grounded reinforcement finetuning. *arXiv preprint arXiv:2505.19702*, 2025. 2, 3
- [33] OpenAI. Gpt-4o mini: advancing cost-efficient intelligence. <https://openai.com/index/gpt-4o-mini-advancing-cost-efficient-intelligence/>, 2024. 5
- [34] OpenAI. Openai-o3. <https://openai.com/index/introducing-o3-and-o4-mini/>, 2025. 6
- [35] Yingzhe Peng, Gongrui Zhang, Miaosen Zhang, Zhiyuan You, Jie Liu, Qipeng Zhu, Kai Yang, Xingzhong Xu, Xin Geng, and Xu Yang. Lmm-rl: Empowering 3b llms with strong reasoning abilities through two-stage rule-based rl. *arXiv preprint arXiv:2503.07536*, 2025. 2
- [36] Maurice Ptito, Maxime Bleau, and Joseph Bouskila. The retina: a window into the brain, 2021. 1
- [37] Hao Shao, Shengju Qian, Han Xiao, Guanglu Song, Zhuofan Zong, Letian Wang, Yu Liu, and Hongsheng Li. Visual cot: Advancing multi-modal language models with a comprehensive dataset and benchmark for chain-of-thought reasoning. *Advances in Neural Information Processing Systems*, 37:8612–8642, 2024. 2, 3
- [38] Zhihong Shao, Peiyi Wang, Qihao Zhu, Runxin Xu, Junxiao Song, Xiao Bi, Haowei Zhang, Mingchuan Zhang, YK Li, Yang Wu, et al. Deepseekmath: Pushing the limits of mathematical reasoning in open language models. *arXiv preprint arXiv:2402.03300*, 2024. 3, 5, 6, 7
- [39] Haozhan Shen, Peng Liu, Jingcheng Li, Chunxin Fang, Yibo Ma, Jiajia Liao, Qiaoli Shen, Zilun Zhang, Kangjia Zhao, Qianqian Zhang, et al. Vlm-rl: A stable and generalizable rl-style large vision-language model. *arXiv preprint arXiv:2504.07615*, 2025. 2, 3
- [40] Baifeng Shi, Boyi Li, Han Cai, Yao Lu, Sifei Liu, Marco Pavone, Jan Kautz, Song Han, Trevor Darrell, Pavlo Molchanov, et al. Scaling vision pre-training to 4k resolution. In *Proceedings of the Computer Vision and Pattern Recognition Conference*, pages 9631–9640, 2025. 2
- [41] Alex Su, Haozhe Wang, Weiming Ren, Fangzhen Lin, and Wenhui Chen. Pixel reasoner: Incentivizing pixel-space reasoning with curiosity-driven reinforcement learning. *arXiv preprint arXiv:2505.15966*, 2025. 2, 3, 5, 6, 7
- [42] Guangyan Sun, Mingyu Jin, Zhenting Wang, Cheng-Long Wang, Siqi Ma, Qifan Wang, Tong Geng, Ying Nian Wu, Yongfeng Zhang, and Dongfang Liu. Visual agents as fast and slow thinkers. *arXiv preprint arXiv:2408.08862*, 2024. 1
- [43] Richard S Sutton, Andrew G Barto, et al. *Reinforcement learning: An introduction*. MIT press Cambridge, 1998. 2
- [44] Huajie Tan, Yuheng Ji, Xiaoshuai Hao, Minglan Lin, Pengwei Wang, Zhongyuan Wang, and Shanghang Zhang. Reason-rl: Reinforcement fine-tuning for visual reasoning. *arXiv preprint arXiv:2503.20752*, 2025. 2
- [45] Gemini Team, Petko Georgiev, Ving Ian Lei, Ryan Burnell, Libin Bai, Anmol Gulati, Garrett Tanzer, Damien Vincent, Zhufeng Pan, Shibo Wang, et al. Gemini 1.5: Unlocking multimodal understanding across millions of tokens of context. *arXiv preprint arXiv:2403.05530*, 2024. 5
- [46] Omkar Thawakar, Dinura Dissanayake, Ketan More, Ritesh Thawkar, Ahmed Heakl, Noor Ahsan, Yuhao Li, Mohammed Zumri, Jean Lahoud, Rao Muhammad Anwer, et al. Llamavol: Rethinking step-by-step visual reasoning in llms. *CoRR*, 2025. 2
- [47] Leandro von Werra, Younes Belkada, Lewis Tunstall, Edward Beeching, Tristan Thrush, Nathan Lambert, Shengyi Huang, Kashif Rasul, and Quentin Gallouédec. Trl: Transformer reinforcement learning. <https://github.com/huggingface/trl>, 2020. 7
- [48] Haochen Wang, Xiangtai Li, Zilong Huang, Anran Wang, Jiacong Wang, Tao Zhang, Jiani Zheng, Sule Bai, Zijian Kang, Jiashi Feng, et al. Traceable evidence enhanced visual grounded reasoning: Evaluation and methodology. *arXiv preprint arXiv:2507.07999*, 2025. 2, 3, 6, 7, 8
- [49] Haozhe Wang, Chao Qu, Zuming Huang, Wei Chu, Fangzhen Lin, and Wenhui Chen. Vl-rethinker: Incentivizing self-reflection of vision-language models with reinforcement learning. *arXiv preprint arXiv:2504.08837*, 2025. 2
- [50] Peng Wang, Shuai Bai, Sinan Tan, Shijie Wang, Zhihao Fan, Jinze Bai, Keqin Chen, Xuejing Liu, Jialin Wang, Wenbin Ge, et al. Qwen2-vl: Enhancing vision-language model’s perception of the world at any resolution. *arXiv preprint arXiv:2409.12191*, 2024. 1
- [51] Wenbin Wang, Liang Ding, Minyan Zeng, Xiabin Zhou, Li Shen, Yong Luo, Wei Yu, and Dacheng Tao. Divide, conquer and combine: A training-free framework for high-resolution image perception in multimodal large language models. In *Proceedings of the AAAI Conference on Artificial Intelligence*, pages 7907–7915, 2025. 7
- [52] Yaoting Wang, Shengqiong Wu, Yuecheng Zhang, Shuicheng Yan, Ziwei Liu, Jiebo Luo, and Hao Fei. Multimodal chain-of-thought reasoning: A comprehensive survey. *CoRR*, abs/2503.12605, 2025. 1, 2
- [53] Penghao Wu and Saining Xie. V?: Guided visual search as a core mechanism in multimodal llms. In *Proceedings of the IEEE/CVF Conference on Computer Vision and Pattern Recognition*, pages 13084–13094, 2024. 7
- [54] Zhiyu Wu, Xiaokang Chen, Zizheng Pan, Xingchao Liu, Wen Liu, Damai Dai, Huazuo Gao, Yiyang Ma, Chengyue Wu, Bingxuan Wang, et al. Deepseek-vl2: Mixture-of-

- experts vision-language models for advanced multimodal understanding. *arXiv preprint arXiv:2412.10302*, 2024. 1
- [55] Yi Yang, Xiaoxuan He, Hongkun Pan, Xiyan Jiang, Yan Deng, Xingtao Yang, Haoyu Lu, Dacheng Yin, Fengyun Rao, Minfeng Zhu, et al. R1-onevision: Advancing generalized multimodal reasoning through cross-modal formalization. *arXiv preprint arXiv:2503.10615*, 2025. 2
- [56] Yuan Yao, Tianyu Yu, Ao Zhang, Chongyi Wang, Junbo Cui, Hongji Zhu, Tianchi Cai, Haoyu Li, Weilin Zhao, Zhihui He, Qianyu Chen, Huarong Zhou, Zhensheng Zou, Haoye Zhang, Shengding Hu, Zhi Zheng, Jie Zhou, Jie Cai, Xu Han, Guoyang Zeng, Dahai Li, Zhiyuan Liu, and Maosong Sun. Minicpm-v: A gpt-4v level mllm on your phone. *CoRR*, abs/2408.01800, 2024. 2
- [57] Jiabo Ye, Haiyang Xu, Haowei Liu, Anwen Hu, Ming Yan, Qi Qian, Ji Zhang, Fei Huang, and Jingren Zhou. mplug-owl3: Towards long image-sequence understanding in multi-modal large language models. *arXiv preprint arXiv:2408.04840*, 2024. 2
- [58] Yufei Zhan, Shurong Zheng, Yousong Zhu, Hongyin Zhao, Fan Yang, Ming Tang, and Jinqiao Wang. Griffon v2: Advancing multimodal perception with high-resolution scaling and visual-language co-referring. In *Proceedings of the IEEE/CVF International Conference on Computer Vision*, pages 22947–22957, 2025. 1, 3
- [59] Yufei Zhan, Yousong Zhu, Shurong Zheng, Hongyin Zhao, Fan Yang, Ming Tang, and Jinqiao Wang. Vision-r1: Evolving human-free alignment in large vision-language models via vision-guided reinforcement learning. *CoRR*, 2025. 2
- [60] Jingyi Zhang, Jiaying Huang, Huanjin Yao, Shunyu Liu, Xikun Zhang, Shijian Lu, and Dacheng Tao. R1-vl: Learning to reason with multimodal large language models via step-wise group relative policy optimization. *CoRR*, abs/2503.12937, 2025. 2
- [61] Renshan Zhang, Rui Shao, Gongwei Chen, Miao Zhang, Kaiwen Zhou, Weili Guan, and Liqiang Nie. Falcon: Resolving visual redundancy and fragmentation in high-resolution multimodal large language models via visual registers. In *Proceedings of the IEEE/CVF International Conference on Computer Vision*, pages 23530–23540, 2025. 2
- [62] Yi-Fan Zhang, Qingsong Wen, Chaoyou Fu, Xue Wang, Zhang Zhang, Liang Wang, and Rong Jin. Beyond llava-hd: Diving into high-resolution large multimodal models. *CoRR*, abs/2406.08487, 2024. 1, 2
- [63] Yi-Fan Zhang, Huanyu Zhang, Haochen Tian, Chaoyou Fu, Shuangqing Zhang, Junfei Wu, Feng Li, Kun Wang, Qingsong Wen, Zhang Zhang, et al. Mme-realworld: Could your multimodal llm challenge high-resolution real-world scenarios that are difficult for humans? *arXiv preprint arXiv:2408.13257*, 2024. 5, 6, 8
- [64] Kesen Zhao, Beier Zhu, Qianru Sun, and Hanwang Zhang. Unsupervised visual chain-of-thought reasoning via preference optimization. *CoRR*, abs/2504.18397, 2025. 2, 3
- [65] Ziwei Zheng, Michael Yang, Jack Hong, Chenxiao Zhao, Guohai Xu, Le Yang, Chao Shen, and Xing Yu. Deep-eyes: Incentivizing "thinking with images" via reinforcement learning. *arXiv preprint arXiv:2505.14362*, 2025. 2, 3, 4, 5, 6, 7
- [66] Jinguo Zhu, Weiyun Wang, Zhe Chen, Zhaoyang Liu, Shenglong Ye, Lixin Gu, Hao Tian, Yuchen Duan, Weijie Su, Jie Shao, et al. Internvl3: Exploring advanced training and test-time recipes for open-source multimodal models. *arXiv preprint arXiv:2504.10479*, 2025. 1, 3, 5, 6, 7, 8